Passivation Effects on Low-Temperature Gettering in Multicrystalline Silicon

Mohammad Al-Amin, *Student Member, IEEE*, and John D. Murphy

***Abstract*—Annealing at ≤ 500 °C changes minority carrier lifetime in as-grown multicrystalline silicon substantially. Part of the change arises from internal gettering of impurities, but surface passivation for lifetime measurement results in additional effects. We report experiments that aim to clarify the role of passivation. Long-term annealing (up to 60 h) is performed on silicon nitride passivated multicrystalline silicon, and lifetime and interstitial iron concentrations are monitored at each processing stage. Lifetime in all samples is improved under certain conditions, with improvements always achieved at 400 °C. Increases are pronounced in low-lifetime bottom samples, with improvement by a factor of 2.7 at 400 °C or 3.8 at 500 °C. Important differences are found compared with our previous study with iodine–ethanol passivation. First, as-received lifetime is higher with silicon nitride not due to a substantial difference in surface recombination. Second, while interstitial iron concentrations often initially increase with iodine–ethanol, they tend to reduce with silicon nitride. Third, lifetime in high-lifetime samples reduces substantially with iodine–ethanol but increases with silicon nitride. Secondary ion mass spectrometry reveals high iron concentrations in annealed silicon nitride. Results are discussed in terms of gettering of impurities to, and bulk passivation arising from, silicon nitride films.**

***Index Terms*—Gettering, iron, multicrystalline, passivation, silicon.**

I. Introduction

MULTICRYSTALLINE silicon (mc-Si) wafers contain crystallographic defects, such as grain boundaries and dislocations, as well as considerable concentrations of transition metal impurities. Metallic impurities exist in many forms, including as point-like defects in the bulk, in precipitates, or bound to dislocations. Most of the transition metals are tied up in precipitates [1], which are strong recombination centers, but per impurity atom are less detrimental to minority carrier lifetime (henceforth just "lifetime") than point-like defects in the bulk [2]. The distribution of defects can be modified by thermal processing to maximize the lifetime.

One approach to improve lifetime is to apply an annealing procedure at low temperatures (≤ 600 °C). At such temperatures, the solubility of many impurities is low; therefore, in theory, such procedures should not result in the release of metals from precipitates in the material, and the risk of external contamination is small. Even at these low temperatures, many free metallic impurities are sufficiently mobile that they are relocated within the photovoltaic (PV) substrate or device. Many studies have been performed into low-temperature annealing of mc-Si [3]–[8], and under certain conditions low-temperature processing can improve lifetime [6], [7], increase cell efficiency [3], [8], and reduce interstitial iron concentration [4], [5]. However, the mechanism underpinning the changes that occur is not fully understood and slight differences in experimental methodologies have been shown to result in substantially different findings.

Our previous work has shown that low-temperature annealing in the absence of a dielectric surface passivation film can improve lifetime in relatively poor mc-Si wafers from the bottom and top of an ingot by redistribution of impurities [6]. Surprisingly, the initial impact on relatively high lifetime wafers from the middle of the ingot was a dramatic reduction in lifetime. In addition, despite the interstitial iron being massively supersaturated at the temperatures used [9], the interstitial iron concentration did not always reduce. In many cases, the impact of low-temperature annealing was to increase the measured interstitial iron concentration, and the interstitial iron changes in sister samples with near identical microstructures did not exhibit a simple temperature dependence. Our findings were in stark contrast with a previous study by Krain *et al*., which used silicon nitride (SiN_x) surface passivation on samples from different height positions of the block [4]. In their study, a systematic reduction in the interstitial iron concentration was found and the activation energy for this process was consistent with that for the diffusion of interstitial iron. This paper aims to address this apparent conflict and to further the understanding of the initial lifetime reduction.

Why might the surface passivation treatment be a relevant issue for low-temperature gettering? SiN_x films deposited by plasma-enhanced chemical vapor deposition (PECVD) at temperatures around 300 to 425 °C are hydrogen rich [10], [11]. There is clear direct evidence for hydrogen entering the bulk from SiN_x films after annealing at temperatures considerably higher than the deposition temperature. For instance, very short (∼1 min) post deposition annealing at 750 °C gives rise to the formation of platinum–hydrogen complexes [10], and deuterium trapped at oxide precipitates is detected by secondary ion mass spectrometry (SIMS) in samples with deuterated SiN_x fired at 800 °C [12]. At lower temperatures, direct evidence of bulk hydrogenation is difficult to obtain due to the lower concentrations involved. However, if hydrogenation does also occur at these temperatures, then it could affect both lifetime and internal

Manuscript received September 20, 2016; revised October 6, 2016; accepted October 10, 2016. Date of publication November 14, 2016; date of current version December 20, 2016. This work was supported in part by the Engineering and Physical Sciences Research Council (EPSRC) under Grant EP/J01768X/2 and Grant EP/M024911/1, the EPSRC Global Challenges Research Fund under Grant EP/P511079/1, and in part by the Royal Society under Grant RG100076. The work of J. D. Murphy was supported by Royal Academy of Engineering/EPSRC Research Fellowship.

The authors are with the School of Engineering, University of Warwick, Coventry CV4 7AL, U.K. (e-mail: m.al-amin@warwick.ac.uk; john.d.murphy@warwick.ac.uk).

Color versions of one or more of the figures in this paper are available online at http://ieeexplore.ieee.org.

Digital Object Identifier 10.1109/JPHOTOV.2016.2618608

gettering of interstitial iron. Furthermore, the possibility of external gettering during the long low temperature annealing procedure should not be excluded. Rinio *et al.*'s study on partially processed cells concluded that external gettering to the emitter was responsible for most of the improvement observed [3]. A recent study by Liu *et al.* has also found iron to be segregated evenly within PECVD SiN_x films on the surface of iron-contaminated single-crystal silicon that has been annealed at 700 °C [13].

Several studies using photoconductance lifetime methods have found that the low-temperature behavior of iron in silicon depends on the surface passivation scheme used [5], [14]–[16]. It is frequently suggested, although not explicitly proven, that this is due to hydrogenation of the bulk from the dielectric. Liu and Sun *et al.* compare the effects of SiO_2, Al_2O_3, and SiN_x passivation on the iron concentration decay kinetics, and find the decay kinetics depend on passivation type [5], [14], [16]. Their results suggest that no or very little hydrogenation occurs from the SiO_2, some hydrogen in-diffuses from Al_2O_3 and substantial hydrogenation occurs from the SiN_x. Other results reported by Karzel *et al.* compare a room temperature quinhydrone–methanol treatment with SiN_x, with the latter introducing hydrogen into the bulk that influences the behavior of interstitial iron [15]. Hydrogenation control in mc-Si is very important, and recent work has shown that it is possible to manipulate the hydrogen charge state [17] as a route to higher lifetimes in PV substrates.

In this paper, we present the results of a comprehensive study that aims to assess the role of surface passivation on low-temperature annealing experiments. In our experiments, we take into account the ingot height position from which the samples were obtained, as this strongly affects the starting lifetime, interstitial iron concentration, and microstructure (particularly the density of grown-in dislocations). Sister samples from each location are passivated with PECVD SiN_x and annealed 300 to 500 °C. Lifetime and interstitial iron concentration are measured at every annealing step with bulk lifetime measurements and with photoluminescence (PL) imaging. SIMS is used to measure the iron distribution in the SiN_x films in certain samples after annealing. The data are compared with our previous work using a temporary iodine–ethanol (I-E) passivation scheme [6] to assess the impact of possible hydrogenation from and gettering to the SiN_x film.

II. Experimental Methods

The key processing and characterization steps used are summarized in Fig. 1.

A. Sample Selection

As-cut multicrystalline wafers (156 mm × 156 mm × 200 μm) were sourced from four different height positions [top (T), top middle (MT), bottom middle (MB) and bottom (B)] of an edge block of a commercially grown boron-doped ingot. Resistivities were in the range of 4.75–11.5 Ω cm. A single-crystal Czochralski silicon wafer with a resistivity of 8 Ω cm and a thickness of 740 μm was used for control purposes.

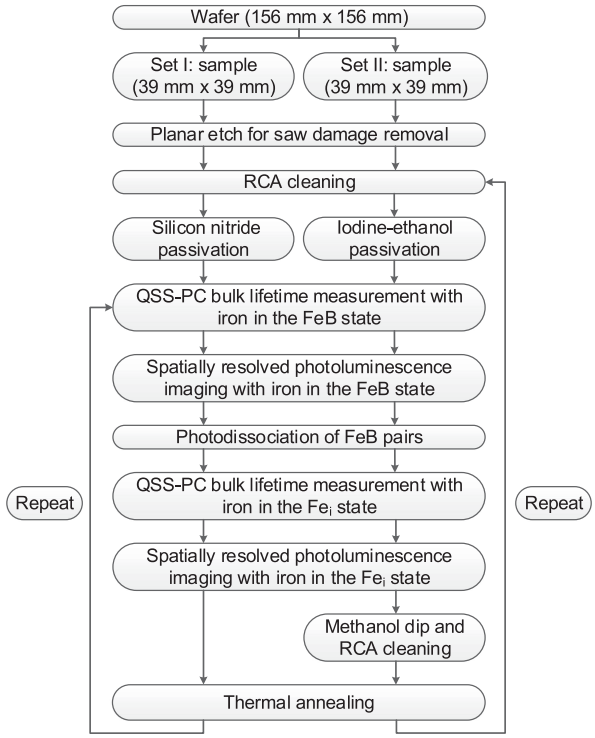

Fig. 1. Processing and characterization sequence for the low-temperature internal gettering experiments.

Wafers were laser cut into 39 mm × 39 mm samples. Set I and Set II samples came from adjacent locations of the wafers. For each set of experiments, sister samples from subsequent wafers with near-identical microstructures were selected for annealing at different temperatures. Dislocation density maps for Set II samples have been published previously [6]. The dislocation density distributions are typical of those found in mc-Si, being highest at the top and lowest at the bottom.

B. Surface Passivation and Lifetime Measurement

Samples were first chemically polished with a planar etch solution comprising HF (50%), HNO_3 (69%), and CH_3COOH (100%) in the ratio of 24:58:18 to remove saw damage. Samples, which are then 130 to 140 μm thick, were then subjected to RCA cleaning. Samples from Set I were passivated with ∼70 nm SiN_x grown on both sides by remote PECVD at ∼375 °C at Institut für Solarenergieforschung Hameln (ISFH). This process required the samples to be at the deposition temperature for approximately 10 min. Samples from Set II were passivated with a liquid I-E solution using a method described in [6]. The I-E passivation is only applied at the time of the lifetime measurements and does not involve the sample being heated above room temperature.

Lifetimes were measured at room temperature using quasi-steady-state photoconductance (QSS-PC) [18] with a Sinton WCT-120 lifetime tester. In this paper, we use $\tau_{\mathrm{effective}}$ to denote the measured minority carrier lifetime with iron in the iron–boron (FeB) state, and where a single value is reported, it is the value at an excess carrier concentration of 1×10^{15} cm^{-3}. In order to measure the bulk interstitial iron concentration,

FeB pairs were dissociated by more than 50 consecutive intense flashes (∼30 suns) of light with ∼10 μs decay constant. Interstitial iron concentrations were determined from the lifetime change that occurs when FeB complexes are dissociated using the approach detailed previously [19]. More details about error considerations and detection limits are given in our previous publication [6]. For some purposes in this paper, we refer to the effective lifetime due to recombination other than FeB pairs in the bulk. We define this according to $\tau_{\rm other} = (\frac{1}{\tau_{\rm effective}} - \frac{1}{\tau_{\rm FeB}})^{-1}$ and calculate $\tau_{\rm FeB}$ (the lifetime due to recombination of FeB pairs) at each step using the Shockley–Read–Hall recombination parameters for FeB of Rein and Glunz [20].

The spatial distribution of lifetime was measured with bulk iron in the FeB and Fe_i state using a BT Imaging LIS-L1 PL imaging system. PL images were acquired with excitation by LEDs with a wavelength of 650 nm and these were calibrated using the lifetime from QSS-PC [21]. All the lifetime images presented in this paper are with iron in the FeB state and with ∼160 μm pixel size. The spatial distribution of interstitial iron concentration was calculated from lifetime and excess carrier concentration values at every pixel before and after dissociation of FeB pairs, as reported in Macdonald *et al*. [22]. Lower injection was used than in the bulk average measurement to avoid unwanted dissociation of FeB pairs during measurement.

C. Low-Temperature Annealing

Three sister samples for each of Set I and Set II from every height position were annealed at 300, 400, and 500 °C. SiN_x passivation remains on the Set I samples during annealing. After each annealing step, samples were stored in the dark for ≥ 36 h to ensure complete reassociation of FeB defects [23], prior to recharacterization by QSS-PC and PL imaging.

D. Secondary Ion Mass Spectrometry Iron Measurements

SIMS was performed through the SiN_x film and into the bulk of the three Set I samples. Measurements were performed by EAG Laboratories on a commercial basis. The measurement depth resolution was < 1.5 nm/step, although the actual resolution was limited by the mixing of bombarded ions during SIMS measurements. Data were collected from a circular area with a diameter of ∼60 μm. The detection limit for iron was $\sim 4 \times 10^{14}\,{\rm cm}^{-3}$. Silicon was monitored as a marker species with its secondary ion intensity qualitatively measured, which served to distinguish the locations of SiN_x and the Si bulk in the depth profiles. The depth was calibrated using the known thickness of the SiN_x film.

The SIMS depth profiles were taken from regions laser cut out of the bottom samples annealed for the maximum duration (33 h at 300 °C; 25 h at 400 °C; 60 h at 500 °C) in which there was a large reduction ($> 10^{12}$ cm^{-3}) in interstitial iron compared with the initial value. If such a concentration of iron from a 140 μm thick sample is instead distributed in 140 nm of SiN_x (accounting for both sides), the average concentration of iron in the SiN_x would be $> 10^{15}\,{\rm cm}^{-3}$, which would be detectable by SIMS. SIMS is sensitive to total iron; therefore, any non-interstitial iron also gettered from the bulk may also segregate to the SiN_x layer.

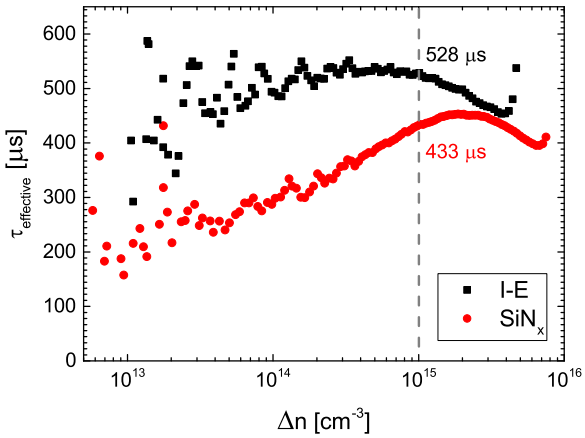

Fig. 2. Injection-dependent lifetime in samples from the same *p*-type Czochralski silicon control wafer (740 μm thick; $1.2 \times 10^{15}\,{\rm cm}^{-3}$ boron) with different passivation schemes. The vertical dashed line and stated values are at $\Delta n = 10^{15}\,{\rm cm}^{-3}$, as used for subsequent measurements on mc-Si.

III. Results

A. Lifetime in Control Samples

Fig. 2 shows the injection dependence of lifetime in the Czochralski silicon control samples taken from the same wafer, which have a similar doping level to the mc-Si samples studied. The lifetime at $\Delta n = 10^{15}\,{\rm cm}^{-3}$ is 433 μs with SiN_x passivation and 528 μs with I-E passivation. On the assumption that the bulk lifetime is the same in both samples after passivation, any difference would be due to different surface recombination velocities. Under this assumption, the surface recombination velocity would be 22% higher in the SiN_x case. It is not possible to give an absolute value for the surface recombination velocity partly because the condition of near-infinite bulk lifetime in the control is not satisfied. Previous work with the same SiN_x passivation scheme on 670 μm thick samples (similar doping, same injection) gives effective lifetimes up to 3.1 ms [19]. This puts an upper limit on the surface recombination velocity at around 11 cm/s for the SiN_x scheme used here. A value for I-E lower than this is consistent with the literature [24].

B. Bulk Lifetime and Interstitial Iron Data

QSS-PC lifetime and interstitial iron measurements for the Set I samples passivated with SiN_x are shown in Figs. 3 and 4, respectively. Data are shown for the four ingot height positions, and sister samples at each position were annealed at either 300, 400, or 500 °C for the cumulative annealing time shown. A summary of the ultimate effects of low-temperature annealing on the samples studied is given in Table I. In addition, given in Table I are values of $\tau_{\rm other}$ in the as-received samples with both passivation types. The SiN_x surface passivation did not degrade dramatically upon annealing. If a small degradation did occur, then the impact of low-temperature annealing on the true bulk lifetime is actually more significant than we have reported. We note that it is not easily possible to use

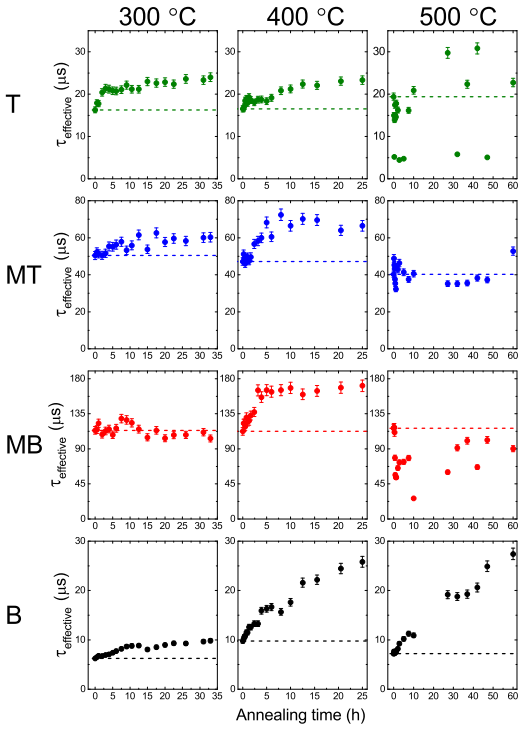

Fig. 3. Lifetime in Set I samples with SiN_x surface passivation measured by QSS-PC at an injection level of 1×10^{15} cm^{-3} for samples from the top (T), top middle (MT), bottom middle (MB), and bottom (B) of the ingot. Sister samples were annealed at 300 °C, 400 °C, and 500 °C for the cumulative annealing time plotted. The dashed lines represent the as-grown values.

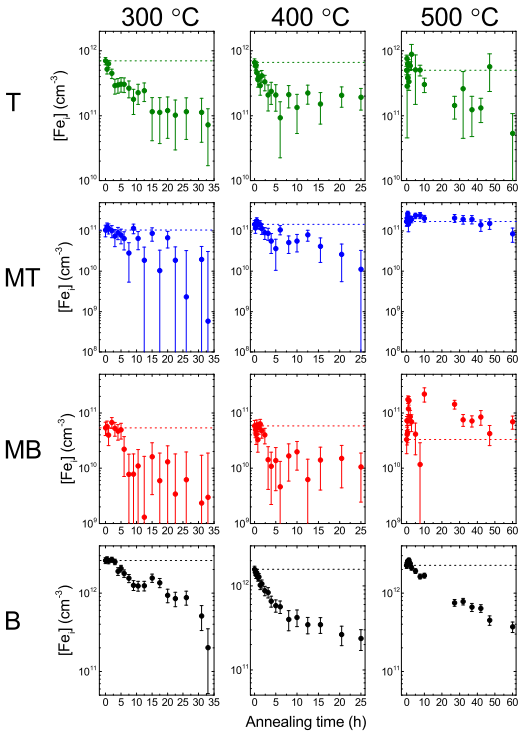

Fig. 4. Bulk interstitial iron concentration ([Fe_i]) in Set I samples (SiN_x passivation) for samples from the top (T), top middle (MT), bottom middle (MB), and bottom (B) of the ingot. Sister samples were annealed at 300 °C, 400 °C, and 500 °C for the cumulative annealing time plotted. The dashed lines represent the initial values.

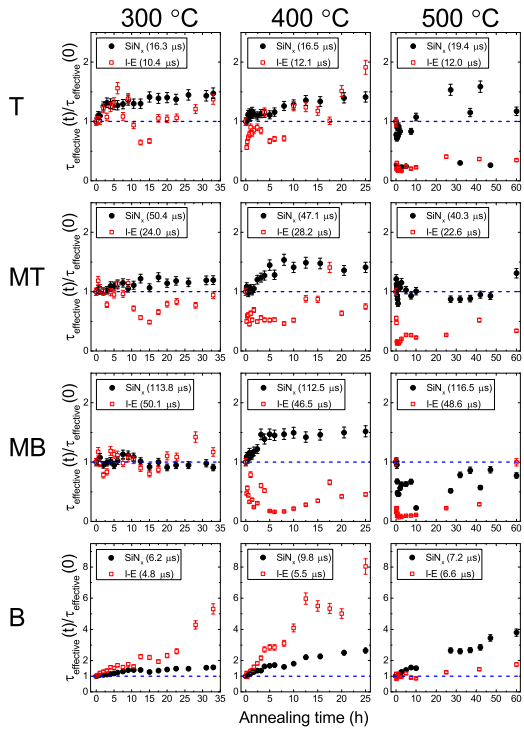

Fig. 5. Comparison in normalized lifetime with iron in the FeB state for the Set I (SiN_x) and Set II (I-E) samples from the top (T), top middle (MT), bottom middle (MB), and bottom (B) of the ingot. Samples from every set were annealed at 300 °C, 400 °C, and 500 °C for the cumulative annealing time plotted. The lifetimes were measured at an injection level of 1×10^{15} cm^{-3}. The values in the brackets represent the as-grown lifetime. The dashed lines represent the starting states.

control samples to monitor low-temperature annealing effects on surface recombination, as the bulk lifetime in float-zone silicon can degrade substantially [25] and thermal donors form in Czochralski silicon toward the top of the temperature range we have investigated.

Fig. 5 shows a comparison in lifetime normalized to the starting value for the Set I (SiN_x passivated) and Set II (I-E passivated) samples for samples from all height positions annealed at 300, 400, or 500 °C for the cumulative annealing time shown. Fig. 6 shows the corresponding comparison between Set I and Set II for interstitial iron concentration. Absolute data for Set II samples have been published previously [6].

Spatially resolved lifetime measurements were performed after every annealing step, with images acquired with iron in the form of FeB pairs, as well as interstitial form. Lifetime images with iron in the FeB state are shown in Fig. 7 for selected sample types and annealing times. The two left columns show a comparison between bottom samples annealed at 400 °C with either I-E or SiN_x passivation. The right two columns show a similar comparison for bottom middle sample. Maps of the interstitial iron concentration distribution for the same conditions are shown in Fig. 8.

C. *Secondary Ion Mass Spectrometry Depth Profiles*

Data from the SIMS measurements are presented in Fig. 9. The top plot shows the secondary ion intensity, which was used

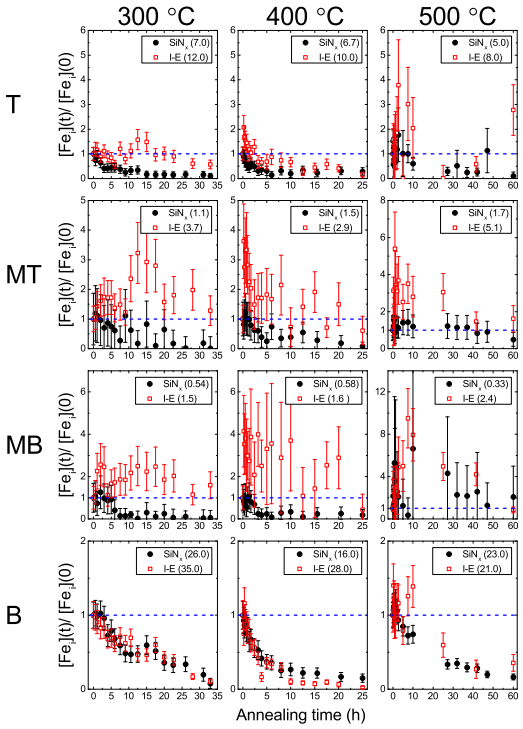

Fig. 6. Comparison in normalized interstitial iron concentration for the Set I (SiN_x) and Set II (I-E) samples from the top (T), top middle (MT), bottom middle (MB), and bottom (B) of the ingot. Samples were annealed at 300 °C, 400 °C, and 500 °C for the cumulative annealing time plotted. The values in the brackets are the interstitial iron concentrations ($\times 10^{11}$ cm^{-3}) for as-grown samples. The dashed lines represent the starting states.

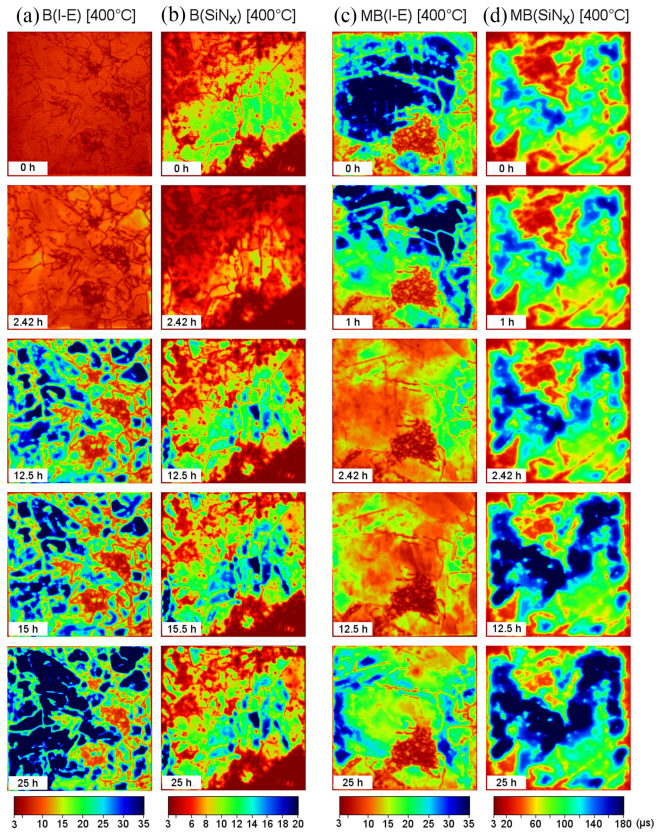

Fig. 7. Spatial distribution of lifetime with iron in the FeB state in selected 39 mm × 39 mm samples. Samples were annealed at the temperatures and cumulative times shown and were sourced from the bottom (B), bottom middle (MB) of a mc-Si block passivated with I-E and PECVD SiN_x. Fig. 8 shows corresponding interstitial iron maps.

to estimate the position of the SiN_x film. The bottom plot shows the iron concentration as a function of depth. A thin (∼20 nm) layer of contamination was found at the surface of each sample. This is likely to have accumulated during the 18 separate annealing and characterization steps. Whilst care was taken to minimize contamination, SiN_x passivated samples could not be RCA cleaned after passivation to avoid damage to the SiN_x film.

Substantial concentrations of iron were always found in the SiN_x film. The concentration was highest nearest the sample surface and reduced with depth into the sample. Neither a spike nor a dip in iron concentration was observed at the interface between SiN_x and the mc-Si bulk. The concentration of iron in the SiN_x was dependent on the annealing temperature, with average concentrations being 2.0×10^{17} cm^{-3} at 500 °C, 4.0×10^{16} cm^{-3} at 400 °C, and 1.7×10^{16} cm^{-3} at 300 °C. The iron concentration just beneath the mc-Si surface was above the SIMS detection limit in all cases, being very high ($> 10^{16}$ cm^{-3}) in the 500 °C case.

IV. Discussion

We do not repeat the discussion regarding the low-temperature gettering effect observed in our previous publication [6] in which data for Set II samples were presented. Here, we discuss only new findings and key differences between the results of the two sets of experiments.

A. Empirical Lifetime Changes in Silicon Nitride Passivated Samples

Our data show that long low temperature annealing can improve the lifetime in as-received mc-Si passivated with SiN_x. Fig. 3 shows that the effective lifetime in such Set I samples from all block locations was increased by annealing at 400 °C. The improvement was particularly significant in bottom samples, which experienced lifetime increases of a factor of ∼2.7. Annealing SiN_x passivated samples at 300 °C had a smaller positive effect on lifetime in all cases except for the bottom middle samples that were unaffected. The effect of annealing at 500 °C was mixed. The biggest relative improvement for any sample was achieved by annealing bottom samples at 500 °C with an improvement of a factor of 3.8 realized by annealing for 60 h. Annealing relatively high lifetime bottom middle samples at 500 °C results in a reduction in lifetime, and the trend in top sample was unclear.

The reason for differences in behavior between 400 and 500 °C is unclear. It is possible that some defects in the bulk dissociate during annealing at the higher temperature and these have a detrimental effect on lifetime in some cases. It is also possible that the SiN_x surface passivation is starting to degrade in an uncontrolled way upon annealing at 500 °C, but this is less likely as the lifetime does recover after a few steps.

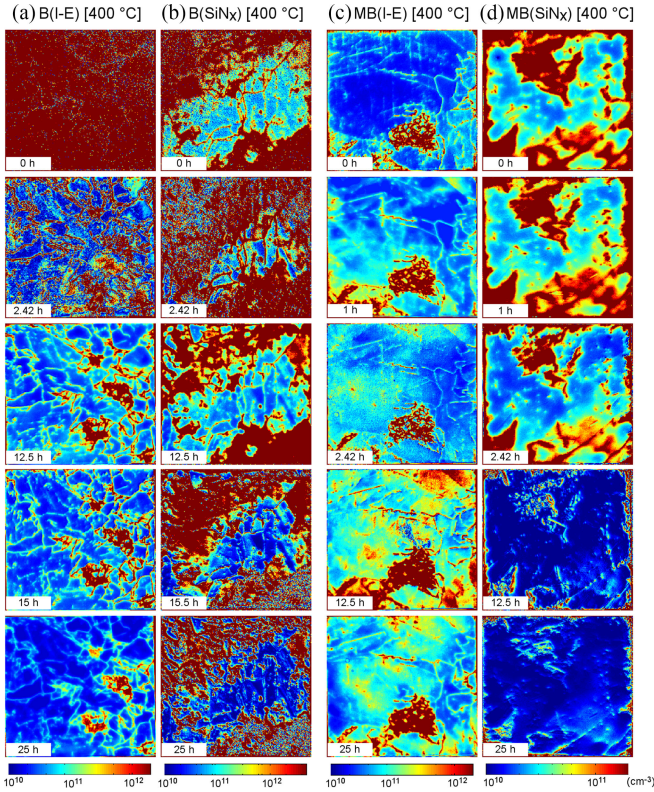

Fig. 8. Spatial distribution of interstitial iron in the same samples for which lifetime measurements are shown in Fig. 7. Samples measuring 39 mm × 39 mm were sourced from the bottom (B) and bottom middle (MB), passivated with I-E or PECVD SiN_x, and annealed at the temperatures and for the cumulative times shown.

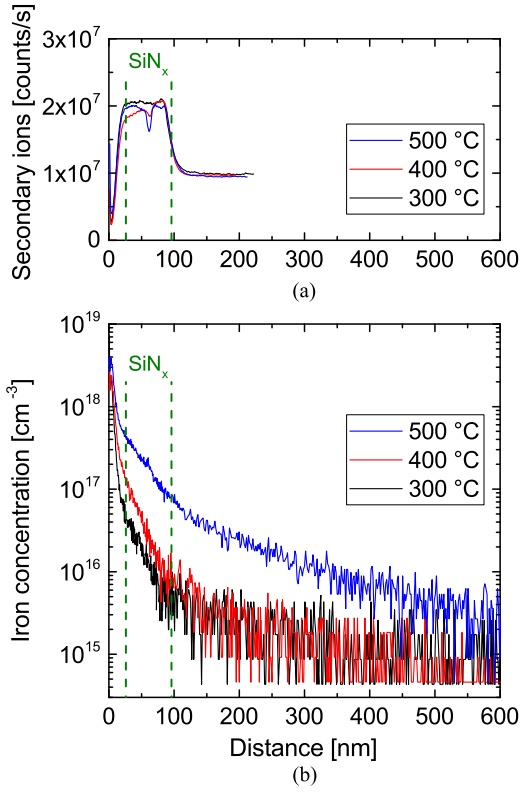

Fig. 9. SIMS depth profiles from bottom samples annealed at 300 °C, 400 °C, or 500 °C from Set I after the final annealing stage. (a) Secondary ion intensity that is used to locate the SiN_x film, the approximate extrema of which are marked as vertical dashes. (b) Concentration measured in the SiN_x film as well as the top part of the mc-Si bulk. The detection limit was $\sim 4 \times 10^{14}$ cm^{-3}. The ~20 nm region nearest the surface is likely due to process contamination.

Only very limited data on the effect of low-temperature annealing on lifetime in SiN_x passivated mc-Si are available in the literature. Liu *et al.* studied the effect of 400 °C annealing on mc-Si achieved an ~2.6 times improvement in lifetime in 5.6 h [14], although the actual values of effective lifetime measured were considerably lower than ours. The PL images of lifetime reported by Krain *et al.* are also qualitatively consistent with our lifetime images reported in Fig. 7(b).

B. Interstitial Iron Changes in Silicon Nitride Passivated Samples

In our mc-Si samples, interstitial iron is highly supersaturated at the annealing temperatures used. Solubility data are not available at low temperatures, but extrapolation of higher temperature trends gives the solubility between 2×10^7 cm^{-3} [26] and $\sim 2 \times 10^9$ cm^{-3} [9], [27] at 500 °C and lower at other temperatures. Our starting interstitial iron concentrations are several orders of magnitude higher than this. It is not, therefore, surprising that the interstitial iron concentration in SiN_x passivated mc-Si has a tendency to reduce on annealing at 300 and 400 °C (see Fig. 4), as there is a driving force to form iron-containing precipitates.

In our previous study, using I-E passivation [6], we compared our iron decay data with those of Krain *et al.* [4], finding our studies not to be quantitatively consistent. We offered two possible explanations for this: 1) hydrogenation from their SiN_x affecting the behavior of interstitial iron and/or 2) that their samples came from different parts of the ingot, so probably have different microstructures. The decay in interstitial iron concentration is clearest in bottom samples as these have the highest concentration, and Fig. 6 shows that in these samples the decay rates are similar for both passivation schemes we have used. Thus, we conclude that hydrogenation (if it occurs) does not explain the difference between the studies and favor the remaining explanation of microstructural differences among the samples. If this is true then the correlation between the temperature dependence of gettering and iron diffusivity found by Krain *et al.* is likely to have been coincidental.

C. Differences Between Iodine–Ethanol and Silicon Nitride Passivation Initial States

Initial lifetimes measured with SiN_x passivation are considerably higher than with I-E passivation (see Table I). Lifetime measurements made on the Cz-Si control sample (see Fig. 2) demonstrate that this is not due to differences in the surface recombination velocity. The comparison samples are from adjacent locations of the same wafers, and although small differences due to slightly different microstructures might occur, they cannot account for the magnitude of the differences observed. We therefore conclude that the *bulk* lifetimes are affected by the

TABLE I
SUMMARY OF STARTING AND FINAL LIFETIMES AND INTERSTITIAL IRON CONCENTRATIONS, AND THEIR RELATIVE VALUES AFTER THE FINAL ANNEALING STAGE.

Ingot position	Annealing temperature (°C)	Total annealing time (h)	As-grown $\tau_{effective}(0)$ (μs)		As-grown $[Fe_i](0)$ ($\times 10^{11}$ cm^{-3})		As-grown $\tau_{other}(0)$ (μs)		Improvement in $\frac{\tau_{effective}(t_{max})}{\tau_{effective}(0)}$		Reduction in $\frac{[Fe_i](0)}{[Fe_i](t_{max})}$	
			SiN_x	I-E	SiN_x	I-E	SiN_x	I-E	SiN_x	I-E	SiN_x	I-E
T	300	33	16.3	10.4	7.0	11.6	29.2	18.5	1.48	1.37	9.66	1.74
	400	25	16.5	12.1	6.7	10.1	28.8	21.9	1.41	1.91	3.45	6.39
	500	60	19.4	12.0	5.0	8.0	31.4	18.3	1.17	0.35	9.34	0.36
MT	300	33	50.4	24.0	1.1	3.7	62.7	34.2	1.20	0.94	10.19	0.78
	400	25	47.1	28.2	1.4	2.9	63.2	39.4	1.41	0.75	12.96	1.65
	500	60	40.3	22.6	1.7	5.1	53.9	37.6	1.31	0.34	2.01	0.62
MB	300	33	113.8	50.1	0.54	1.5	147.3	67.5	0.91	1.17	17.94	0.63
	400	25	112.5	46.5	0.58	1.6	147.5	62.0	1.52	0.46	5.51	0.35
	500	60	116.5	48.6	0.33	2.4	135.9	81.6	0.78	1.00	0.48	1.18
B	300	33	6.4	4.8	26.1	35.0	14.9	10.7	1.58	5.31	12.94	9.41
	400	25	9.8	5.5	15.8	28.0	21.9	12.0	2.65	8.03	6.69	22.95
	500	60	7.2	6.6	22.5	20.8	17.5	12.7	3.80	1.76	6.06	2.81

The red or green shading represent deterioration or improvement in bulk carrier lifetime, or an increase or decrease in the interstitial iron concentration, respectively.

choice of surface passivation technique, and possible reasons for this are discussed later.

The starting values of interstitial iron concentration are dependent on the choice of passivation method (Table I) with concentrations usually considerably lower with SiN_x passivation compared with I-E passivation. This finding is consistent with the study of Karzel *et al.* [15], whose quinhydrone–methanol solution is similar to our I-E solution in that it is a room temperature treatment and probably does not introduce hydrogen into the material. Karzel *et al.* offered possible explanation in terms of hydrogen from SiN_x passivation affecting the interstitial iron concentration, as well as the diffusivity of interstitial iron. Theoretical calculations suggest that hydrogen does not passivate interstitial iron [28], although experimental results suggest that hydrogen may interact with iron under certain conditions [29]–[31]. One additional possibility raised by our SIMS data showing iron incorporation into the SiN_x is that interstitial iron is gettered to the SiN_x layer during the passivation treatment that involves 375 °C annealing for ∼10 min. The kinetic feasibility of this can be assessed using a double-sided diffusion model described in [9] using the established diffusivity for interstitial iron [26]. The biggest absolute difference in as-received interstitial iron levels occurs in bottom samples annealed at 400 °C (see Table I). Taking the true starting interstitial iron concentration to be that measured with I-E passivation, modeling the interstitial iron diffusion to both surfaces shows that 10 min at 375 °C results in an average bulk interstitial iron concentration similar to that measured with SiN_x. Thus, iron gettering to the SiN_x passivation film during the passivation treatment is kinetically viable in this case, and this possibility for the discrepancy between passivation methods is worthy of future investigation.

The difference in starting lifetimes between the I-E and SiN_x passivated samples is not just due to the differences in interstitial iron levels. The values of τ_{other} given in Table I have the lifetime due to recombination at bulk iron factored out and are always substantially higher in the SiN_x case. All we can claim for certain is that SiN_x does something different to the bulk lifetime than I-E. The origin of this difference is not clear from our study alone. Possible explanations might include bulk hydrogenation by passivation (which has been directly proven to occur at higher temperatures [10], [12]) or gettering of impurities other than bulk iron to the SiN_x film.

D. Comparison of Annealed Iodine–Ethanol and Silicon Nitride Passivated Samples

As shown in Figs. 5 and 6, in some circumstances, the low temperature annealing behavior is radically different between the I-E and SiN_x samples, and in other circumstances, it is qualitatively similar. As a general rule, annealing SiN_x passivated mc-Si from all block locations at 300 or 400 °C has a positive effect on lifetime, whereas in the I-E case, the effect is more mixed and can be highly detrimental.

Bottom samples with a relatively low starting lifetime and relatively high starting interstitial iron concentration experience lifetime improvements and longer term interstitial iron reductions with both passivation types. The kinetics of the decay in interstitial iron concentration at a given temperature are very similar in both sets of bottom samples (see Fig. 6), which suggests that the main sink for interstitial iron is the same for both passivation types. This is perhaps surprising given that the samples for SiN_x and I-E passivation for a given annealing temperature were not sister, but adjacent, samples. They therefore have similar properties by virtue of their ingot location by not not near-identical microstructures. For the 400 °C case, Fig. 7(a) and (b) and Fig. 8(a) and (b) show the lifetime and interstitial iron maps, respectively. With both passivation types, the lifetimes increase with annealing and the interstitial iron concentrations decrease. The changes that occur are slow: much slower than if diffusion-limited internal gettering of interstitial iron is the only process involved. The gettering process requiring the longest impurity diffusion length would be gettering to

the SiN_x film (or surface in the case of I-E passivation), yet if known diffusion coefficients of interstitial iron [26] are used with a two-sided surface diffusion calculation [9], the decay in interstitial iron would be faster than observed experimentally by a factor of ~6 at 300 °C and ~15 at 400 °C. At 500 °C, after an initial increase, the decay is slower at 400 °C, which is indicative of multiple mechanisms of iron gettering. This is discussed in Section IV-F.

However, there are good reasons not to abandon the surface or SiN_x film gettering mechanism in bottom samples entirely. Factors in favor include the SIMS data for SiN_x samples, the same interstitial iron decay in non-sister samples, and previous studies that have found iron gettering to free surfaces in single-crystal silicon [32], [33]. Trapping of interstitial iron at crystal defects in mc-Si could slow down the effective diffusion process of interstitial iron, and iron release from elsewhere in the material at 500 °C could complicate the kinetics further.

The time dependence of interstitial iron and lifetime in samples from the middle of the ingot is strongly passivation dependent. The abrupt reduction in lifetime observed in relatively high-lifetime samples with I-E passivation [6] was rarely observed in the SiN_x case. For example, the lifetime in bottom middle samples reduced from 46.5 to just 7.6 μs after 6 h at 400 °C with I-E passivation, whereas the same treatment with SiN_x passivation increases lifetime from 112 to 163 μs. Lifetime images for this sample type are shown in Fig. 7(c) and (d), with the intermediate low-lifetime stage clearly visible with I-E but not with SiN_x passivation. Although the lifetime reduction in the case of I-E passivation is accompanied by an increase in interstitial iron concentration, this increase is far too small to account for the dramatic lifetime reduction. Why does lifetime reduce substantially with I-E but not with SiN_x? One possibility is that bulk passivation from the SiN_x film somehow prevents the formation of the recombination centers that form with I-E passivation. Other possibilities include the case where fast diffusing impurities are released from locations within the bulk of the material upon initial annealing and are gettered by the SiN_x film but not by a free surface or that contamination from outside the sample can enter in the I-E case but not in the SiN_x case as the film might act as a diffusion barrier. The subtleties observed in middle samples are probably masked in bottom samples in which more dominant effects arise from higher impurity concentrations.

E. Gettering of Iron to Silicon Nitride Layers

Our SIMS results (see Fig. 9) show that a high concentration of iron exists in the SiN_x film after annealing. As in the recent study of Liu *et al.* [13], no peak in iron signal was observed at the interface between the SiN_x and the silicon bulk, which demonstrates that the interface itself is not a site for gettering or iron precipitation. The iron profile through the SiN_x is also fairly smooth (no large spikes), which suggests that iron has segregated throughout the SiN_x and does not exist in large precipitates. (The step size for SIMS depth profiling was < 1.5 nm, and therefore, large precipitates would be detectable in principle.)

The concentrations of iron found in the SiN_x layer are higher than expected if the only source of iron were interstitial iron lost from the bulk. The area selected for SIMS analysis was known from PL imaging experiments to have interstitial iron reductions of up to $\sim 2 \times 10^{12}\,\mathrm{cm}^{-3}$; therefore, if all this were gettered to the SiN_x the concentration in the SiN_x would be $\sim 2 \times 10^{15}\,\mathrm{cm}^{-3}$. Fig. 9(b) shows substantially higher iron concentrations in the SiN_x than this. The additional iron could come from iron-containing precipitates in the bulk, which in mc-Si are well known to contain more iron than that is dissolved in the bulk [1]. The possibility that some of the iron comes from contamination cannot be ruled out, but it is noted that the levels of iron beneath the mc-Si surface are well in excess of the expected solid solubility of interstitial iron [9], [26], [27] at the annealing temperatures used. Our results unambiguously show that iron is highly soluble in SiN_x films processed at low temperatures, regardless of the origin of the iron. The absence of any interface effects suggests that iron would enter the SiN_x from the mc-Si as well as from the surface of the sample. The recent SIMS study on float-zone silicon by Liu *et al.* [13] compared samples with and without bulk iron contamination, finding much higher concentrations in the SiN_x in the former case. Iron gettering to SiN_x films is therefore an important consideration in the processing of SiN_x passivated silicon solar cells.

F. Complexities of Low-Temperature Gettering in Multicrystalline Silicon

Our results and those of others show that low-temperature gettering in mc-Si is a complex problem. An interstitial iron diffusion limited internal gettering model (as suggested by Krain *et al.* [4]) does not explain all our observations presented here and previously [6]. Specifically, it cannot explain why the reduction in interstitial iron is so slow, why interstitial iron levels sometimes increase in spite of apparent supersaturation, and why we observe slower decays in interstitial iron at 500 °C than at 400 °C. Surface passivation does influence the low-temperature gettering behavior, but not in a straightforward way. Whilst it is tempting to state that hydrogenation from SiN_x is responsible for any differences, we have no direct evidence for this. Our SIMS data and the recent study of Liu *et al.* [13] show that iron is highly soluble in PECVD SiN_x and, given the slow decays in our work (and those of Krain *et al.* [4]), external gettering of interstitial iron at low temperatures is a very important consideration. There are, however, differences between the two passivation schemes (such as why the lifetime in high-lifetime middle samples is more stable with SiN_x than with I-E) that external gettering of interstitial iron cannot easily explain. Possible hydrogenation from PECVD SiN_x at low temperatures ($\leq$ 500 °C) is an important topic for direct future experimentation.

We summarize that at least the following six possible competing mechanisms must be understood to explain low-temperature gettering in mc-Si:

1) internal gettering, whereby impurities diffuse to sites in the material (e.g., grain boundaries, precipitates, or dislocations);
2) defect reconfiguration, whereby defects change state without long-range transport, which could include transformation of one point-like defect into another;

3) external gettering of impurities, whereby impurities diffuse to a layer at the surface (e.g., SiN_x) or the surface itself;
4) bulk passivation of defects, whereby a species, such as hydrogen, could diffuse into the material and changes the recombination activity of defects;
5) changes in the surface recombination velocity, whereby the properties of the interface between silicon and the passivating layer/substance occur;
6) contamination from outside of the sample, whereby impurities undesirably enter the material in an uncontrolled manner.

Importantly, several of the above mechanisms are highly dependent on the specific properties of the mc-Si wafer processed. Empirically, we have established that all as-received mc-Si sample types studied can be improved under the right conditions. However, just as is the case with higher temperature phosphorus diffusion gettering [34], to maximize the benefit the temperature and time should be tailored to the wafer type processed.

V. Conclusion

We have performed a comprehensive study into the effects of low-temperature annealing (300 to 500 °C) on minority carrier lifetime and interstitial iron concentration in as-received mc-Si wafers. We take into account ingot height position (which influences microstructure) and initial properties, and we have used two different passivation schemes (I-E and SiN_x). Under certain conditions, substantial lifetime improvements have been demonstrated in all sample types studied using either passivation scheme. With the more cell-relevant SiN_x passivation scheme, annealing relatively poor bottom samples at 500 °C for 60 h can improve lifetime from 7.2 to 27.5 μs. Annealing at 400 °C for 25 h can improve lifetime in middle samples from 113 to 171 μs and in top samples from 16.5 to 23.3 μs.

The effect of low-temperature annealing on both lifetime and interstitial iron is complex, and depends upon passivation type. Starting lifetimes and interstitial iron concentrations depend on the choice of passivation scheme, as does the subsequent behavior with low-temperature annealing. Substantial lifetime reductions observed after short anneals when measured with I-E passivation are not found in the SiN_x case, therefore, it appears that SiN_x offers more lifetime stability. The possibility that this is due to bulk passivation (perhaps by hydrogen) is not excluded by our results. Importantly, we show, for the first time, that substantial concentrations of iron exist in the SiN_x film after low-temperature annealing. We suggest that gettering of interstitial iron (and probably other impurities) to the SiN_x film is an important consideration that has usually been overlooked in previous studies.

Acknowledgment

The authors are grateful to Dr. K. Bothe at ISFH, Germany, for his assistance in passivating samples with silicon nitride. Data published in this article can be freely downloaded from http://wrap.warwick.ac.uk/82091/.

References

[1] D. Macdonald, A. Cuevas, A. Kinomura, Y. Nakano, and L. J. Geerligs, "Transition-metal profiles in a multicrystalline silicon ingot," *J. Appl. Phys.*, vol. 97, 2005, Art. no. 033523.
[2] W. Kwapil, J. Schön, W. Warta, and M. C. Schubert, "Carrier recombination at metallic precipitates in p-and n-type silicon," *IEEE J. Photovolt.*, vol. 5, no. 5, pp. 1285–1292, Sep. 2015.
[3] M. Rinio *et al.*, "Improvement of multicrystalline silicon solar cells by a low temperature anneal after emitter diffusion," *Progress Photovolt.: Res. Appl.*, vol. 19, pp. 165–169, 2011.
[4] R. Krain, S. Herlufsen, and J. Schmidt, "Internal gettering of iron in multicrystalline silicon at low temperature," *Appl. Phys. Lett.,* vol. 93, 2008, Art. no. 152108.
[5] A. Y. Liu and D. Macdonald, "Precipitation of iron in multicrystalline silicon during annealing," *J. Appl. Phys.*, vol. 115, 2014, Art. no. 114901.
[6] M. Al-Amin and J. D. Murphy, "Increasing minority carrier lifetime in as-grown multicrystalline silicon by low temperature internal gettering," *J. Appl. Phys.*, vol. 119, 2016, Art. no. 235704.
[7] Y. Boulfrad, A. Haarahiltunen, H. Savin, E. J. Øvrelid, and L. Arnberg, "Enhanced performance in the deteriorated area of multicrystalline silicon wafers by internal gettering," *Progress Photovolt.: Res. Appl.*, vol. 23, pp. 30–36, 2015.
[8] M. D. Pickett and T. Buonassisi, "Iron point defect reduction in multicrystalline silicon solar cells," *Appl. Phys. Lett.*, vol. 92, 2008, Art. no. 122103.
[9] J. D. Murphy and R. J. Falster, "The relaxation behaviour of supersaturated iron in single-crystal silicon at 500 to 750°C," *J. Appl. Phys.*, vol. 112, 2012, Art. no. 113506.
[10] S. Kleekajai *et al.*, "Infrared study of the concentration of H introduced into Si by the postdeposition annealing of a SiNx coating," *J. Appl. Phys.*, vol. 106, 2009, Art. no. 123510.
[11] T. Lauinger, J. Moschner, A. G. Aberle, and R. Hezel, "Optimization and characterization of remote plasma-enhanced chemical vapor deposition silicon nitride for the passivation of p-type crystalline silicon surfaces," *J. Vacuum Sci. Technol.*, vol. 16, pp. 530–543, 1998.
[12] G. Hahn, M. Käs, and B. Herzog, "Hydrogenation in crystalline silicon materials for photovoltaic application," *Solid State Phenom.*, vol. 156–158, pp. 343–349, 2010.
[13] A. Y. Liu *et al.*, "Gettering of interstitial iron in silicon by plasma-enhanced chemical vapour deposited silicon nitride films," *J. Appl. Phys.*, 2016, acceped.
[14] A. Liu, C. Sun, and D. Macdonald, "Hydrogen passivation of interstitial iron in boron-doped multicrystalline silicon during annealing," *J. Appl. Phys.*, vol. 116, 2014, Art. no. 194902.
[15] P. Karzel, P. Frey, S. Fritz, and G. Hahn, "Influence of hydrogen on interstitial iron concentration in multicrystalline silicon during annealing steps," *J. Appl. Phys.*, vol. 113, 2013, Art. no. 114903.
[16] C. Sun, A. Liu, S. P. Phang, F. E. Rougieux, and D. Macdonald, "Charge states of the reactants in the hydrogen passivation of interstitial iron in P-type crystalline silicon," *J. Appl. Phys.*, vol. 118, 2015, Art. no. 085709.
[17] P. Hamer, B. Hallam, S. Wenham, and M. Abbott, "Manipulation of hydrogen charge states for passivation of P-type wafers in photovoltaics," *IEEE J. Photovolt.*, vol. 4, no. 5, pp. 1252–1260, Sep. 2014.
[18] R. A. Sinton and A. Cuevas, "Contactless determination of current–voltage characteristics and minority-carrier lifetimes in semiconductors from quasi-steady-state photoconductance data," *Appl. Phys. Lett.*, vol. 69, p. 2510–2512, 1996.
[19] J. D. Murphy, K. Bothe, M. Olmo, V. V. Voronkov, and R. J. Falster, "The effect of oxide precipitates on minority carrier lifetime in p-type silicon," *J. Appl. Phys.*, vol. 110, 2011, Art. no. 053713.
[20] S. Rein and S. W. Glunz, "Electronic properties of interstitial iron and iron-boron pairs determined by means of advanced lifetime spectroscopy," *J. Appl. Phys.*, vol. 98, 2005, Art. no. 113711.
[21] T. Trupke, R. A. Bardos, M. C. Schubert, and W. Warta, "Photoluminescence imaging of silicon wafers," *Appl. Phys. Lett.*, vol. 89, 2006, Art. no. 044107.
[22] D. Macdonald, J. Tan, and T. Trupke, "Imaging interstitial iron concentrations in boron-doped crystalline silicon using photoluminescence," *J. Appl. Phys.*, vol. 103, 2008, Art. no. 073710.
[23] W. Wijaranakula, "The reaction kinetics of iron-boron pair formation and dissociation in p-type silicon," *J. Electrochem. Soc.*, vol. 140, pp. 275–281, 1993.
[24] H. M'saad, J. Michel, J. J. Lappe, and L. C. Kimerling, "Electronic passivation of silicon surfaces by halogens," *J. Electron. Mater.,* vol. 23, pp. 487–491, 1994.

[25] N. E. Grant *et al.*, "Permanent annihilation of thermally activated defects which limit the lifetime of float-zone silicon," *Phys. Status Solidi*, 2016, published online, doi: 10.1002/pssa.201600360.
[26] A. A. Istratov, H. Hieslmair, and E. R. Weber, "Iron and its complexes in silicon," *Appl. Phys. A*, vol. 69, pp. 13–44, 1999.
[27] J. D. Murphy and R. J. Falster, "Contamination of silicon by iron at temperatures below 800°C," *Phys. Status Solidi Rapid Res. Lett.*, vol. 5, pp. 370–372, 2011.
[28] M. Sanati, N. Gonzalez Szwacki, and S. K. Estreicher, "Interstitial Fe in Si and its interactions with hydrogen and shallow dopants," *Phys. Rev. B*, vol. 76,, 2007, Art. no. 125204.
[29] M. Kouketsu and S. Isomae, "Hydrogen passivation of iron-related hole traps in silicon," *J. Appl. Phys.,* vol. 80, pp. 1485–1487, 1996.
[30] S. Leonard, V. P. Markevich, A. R. Peaker, B. Hamilton, and J. D. Murphy, "Evidence for an iron-hydrogen complex in p-type silicon," *Appl. Phys. Lett.*, vol. 107, 2015, Art. no. 032103.
[31] T. Sadoh *et al.*, "Deep level of iron-hydrogen complex in silicon," *J. Appl. Phys.*, vol. 82, pp. 3828–3831, 1997.
[32] X. Gao, H. Mollenkopf, and S. Yee, "Annealing and profile of interstitial iron in boron-doped silicon," *Appl. Phys. Lett.*, vol. 59, pp. 2133–2135, 1991.
[33] T. Heiser and A. Mesli, "How far does the charge state affect the iron behavior in silicon?," *Appl. Phys. Lett.*, vol. 58, pp. 2240–2242, 1991.
[34] J. Hofstetter *et al.*, "Sorting metrics for customized phosphorus diffusion gettering," *IEEE J. Photovoltaics*, vol. 4, no. 6, pp. 1421–1428, Nov. 2014.

Mohammad Al-Amin (S'16) received a BSc. degree in Mechanical Engineering from the Bangladesh University of Engineering and Technology, Bangladesh, in 2005 and a MSc. degree in Sustainable Energy Technologies from University of Southampton, UK in 2010.

From 2010 to 2013, he worked as an Assistant Process Manager at Microsol International and Solon International in Fujairah, UAE, the largest solar cell and module manufacturer in the Middle East. He is currently in the final stages of a Ph.D. degree in Engineering at the University of Warwick, UK. He is also currently an Engineering Tutor at the Coventry University College, UK.

John D. Murphy received an MA in Physics and a DPhil in Materials Science (2006) from the University of Oxford, UK. He was awarded a Royal Academy of Engineering/EPSRC Research Fellowship which he held in Oxford from 2008 to 2013. He moved to a faculty position at the University of Warwick in 2013, where he is now Associate Professor in the School of Engineering. He is Principal Investigator of the EPSRC SuperSilicon PV project which aims to unify the U.K.'s silicon PV materials research activities.